Response to report 4

We thank the referee for the time and effort in reviewing our manuscript. Below we address the conceptual and technical questions posed in their report.

The paper describes that introducing an "impurty" in the hopping can eliminate the so-called the non-Hermitian skin effect. The authors use a transfer-matrix formulation to show the evidence numerically. The authors do not consider a topological insulator but demand the non-Hermitian system to obey the "near-sightedness principle." The numerical evidence that the authors found is actually argued analytically as I show below. I thereby find the authors' claim that the non-Hermitian skin effect is not a topological phenomenon quite unfair. I therefore do not recommend its publication.

We believe that the referee's summary of our work is not completely accurate.

Specifically, the transfer matrix approach presents a rigorous analytical lower bound (Eq. (3)) on the impurity strength that removes the non-Hermitian skin effect, and the numerical diagonalization (Fig. 2) demonstrates that this lower bound holds. Further, we do not "demand that the non-Hermitian system obeys the near-sightedness principle", but rather demonstrate that this principle does not apply, as stated in the title and the abstract.

We thank the referee for sharing the analytical calculation that agrees with our findings in a concrete system. We chose to rely on the transfer matrix approach because unlike the rescaling used by the referee, it applies to any Hamiltonian rather than just the Hatano-Nelson model.

Aside of the above remarks, it appears that the referee considers our claim that the non-Hermitian skin effect is not a topological phenomenon "unfair". Because the notion of topology and topological phenomena are broad and somewhat vague, this is a reasonable concern. Despite that our abstract clearly stated in what sense we consider NHSE not topological, we have now rephrased this claim and state: "we demonstrate that the non-Hermitian skin effect has weaker bulk-edge correspondence than topological insulators". To the best of our knowledge, this fact has not been previously pointed out in the literature.

While we believe that this clarification leaves no room for misunderstanding of our claim, we nevertheless address the rest of the referee's remarks for completeness.

First of all, the authors define the "near-sightedness principle" as the robustness of the insulator, and particularly the topological insulator, against local perturbations. This is because the bulk states of the insulator are localized in real space.

We disagree with this statement. The near-sightedness principle fully applies to band insulators, where all eigenstates are delocalized plane waves according to the Bloch's theorem. That the wave function localization is not a requirement is also stated directly in Kohn's original manuscript (https://doi.org/10.1103/PhysRevLett.76.3168), which we quote here: "The present paper makes a contribution to this effort [of finding O(N) computational methods]. Unlike some other recent work, it does not depend on the existence of well-localized generalized Wannier functions, which exist only in large-gap insulators. It applies to both insulators and metals."

The authors incorrectly extend only the part "topological" to non-Hermitian systems, ignoring the part "insulator" and mistakenly conclude that the non-Hermitian skin effect is not topological because it is not robust against a local change. Since the authors' model originally does not contain any randomness or any other effects to localize bulk states, it is not an insulator and surely does not obey the "near-sightedness principle." If the authors would introduce the randomness as the original Hatano-Nelson model, the conclusion would have been different.

The last statement is incorrect. Because the transfer matrix establishes a lower bound on the wave function growth, Eq. (3) holds also in presence of arbitrary disorder. In the updated version of the manuscript, we added a statement on how the lower bound of Eq. (3) applies to the disordered case.

We also note that the disorder strength at which all eigenstates of the Hatano-Nelson model are localized is the one that does not have a point gap, and thus does not have the non-Hermitian skin effect.

Next, the non-Hermitian skin effect is analytically explained by the introduction of the imaginary gauge transformation, For the Hatano-Nelson model under the open boundary condition, ... Eqs. (R1)-(R13) ... It surely decreases exponentially at the right edge if $(L-1)h < himp$ but increases exponentially up to the hopping impurity. Notice that the conclusion would be different if the eigenvector $\psi H(x)$ for the Hermitian Hamiltonian were localized due to a random potential, and hence the system were indeed an insulator.

We thank the referee for presenting an alternative proof of the collapse of NHSE in the Hatano-Nelson model. We chose the transfer matrix formalism because it applies to arbitrary Hamiltonians.

Finally, the reference list lacks some important papers. Upon introducing the Hatano-Nelson Hamiltonian, the authors do not cite the original Hatano-and-Nelson papers:

- N. Hatano and D.R. Nelson, Phys. Rev. Lett. 77, 570 (1996)

- N. Hatano and D.R. Nelson, Phys. Rev. B 56, 8651 (1997)

The critical papers on the non-Hermitian skin effect and those on the topological property of non-Hermitian systems are lacking too.

- S. Yao and Z. Wang, Phys. Rev. Lett 121, 086803 (2018)

- Z. Gong, Y. Ashida, K. Kawabata, K. Takasan, S. Higashikawa, and M. Ueda, Phys. Rev. X 8, 031079 (2018)

- K. Kawabata, K. Shiozaki, M. Ueda, and M. Sato, Phys. Rev. X 9, 041015 (2019)

Also, the review paper [4] lacks the names of the authors.

We thank the referee for pointing out the missing and incorrectly formatted references. We have fixed these in
the new version of the manuscript.

Response to report 5

We thank the referee for the time and effort in reviewing our manuscript. Below we address the technical and conceptual questions posed in their report.

The authors show that the near-sightedness principle breaks down in the presence of a non-Hermitian impurity. They demonstrate this effect for one- and two-dimensional systems both in the case of a non-Hermitian and Hermitian system. While the effect seems somewhat intuitive, I appreciate that the authors put this effect in the wider context of topological systems.

We thank the referee for their positive assessment.

I have a few questions for the authors about their work:

1. The breakdown of the near-sightedness principle is demonstrated for the one-dimensional system in Fig. 1(a). To show the effect, the authors choose t_R= 0.9 and t_L = 1.1, i.e., the states in the model propagate to the left. The impurity is implemented in such a way that if h_imp ≠ 0 and > 0, t_L becomes smaller and t_R becomes larger. In other words, at the impurity, the states would prefer to move in the opposite direction as compared to the rest of the chain. As such, it is not surprising to me that turning on h_imp > 0, one would at some point find an h_imp

large enough for which all the states will accumulate at the impurity. Did the authors also check whether this effect takes place for h_imp < 0?

Indeed the behavior is quite intuitive, as captured by Eq. (3): when the impurity amplification strength is sufficient to overcome that of the bulk, the states accumulate at the impurity. For that reason h_imp < 0 would not result in the breakdown of NHSE.

---

2. The text in the paper seems to imply that any non-Hermitian impurity would result in a breakdown of the near-sightedness principle. However, this is probably only the case for a non-reciprocal impurity like the one in red in Fig. 1(a). Is that indeed correct?

Indeed, our work demonstrates that given a general bulk Hamiltonian, it is always possible to engineer an impurity that removes NHSE in a system of arbitrary fixed size. As the referee correctly expects, this impurity must be non-reciprocal in order to counteract the non-reciprocal nature of the bulk Hamiltonian.

Lack of near-sightedness principle in non-Hermitian systems

Hélène Spring[1*], Viktor Könye[2], Anton R. Akhmerov[1], and Ion Cosma Fulga[2]

1 Kavli Institute of Nanoscience, Delft University of Technology, P.O. Box 4056, 2600 GA Delft, The Netherlands
2 Institute for Theoretical Solid State Physics, IFW Dresden and Würzburg-Dresden Cluster of Excellence ct.qmat, Helmholtzstr. 20, 01069 Dresden, Germany
*helene.spring@outlook.com

Abstract

The non-Hermitian skin effect is a phenomenon in which an extensive number of states accumulates at the boundaries of a system. It has been associated to nontrivial topology, with nonzero bulk invariants predicting its appearance and its position in real space. Here, we demonstrate that the non-Hermitian skin effect ~~is not a~~ has weaker bulk-edge correspondence than topological ~~phenomenon in general~~insulators: when translation symmetry is broken by a single non-Hermitian impurity, skin modes are depleted at the boundary and accumulate at the impurity site, without changing any bulk invariant. ~~This~~ Similarly, a single non-Hermitian impurity may ~~occur even for~~ deplete the states from a ~~fully~~ region of Hermitian bulk.

In the absence of long-range interactions, local changes made to an insulator have a local effect. This phenomenon is known as the near-sightedness principle: far from the perturbation, the properties of the system remain as they were [1, 2]. Topological insulators, like trivial insulators, obey the near-sightedness principle. The bulk properties of topological insulators stabilize gapless modes at their boundaries in a phenomenon known as bulk-edge correspondence (BEC). symmetry-preserving perturbation at the boundary that destroys the topological phase will locally shift the position of the boundary modes but will not remove them.

In non-Hermitian systems, the near-sightedness principle fails. The spectrum and eigenstates are highly sensitive to boundary conditions: shifting from periodic to open boundary conditions (PBC and OBC) leads to the bulk modes exponentially localizing at the new boundaries [3]. This phenomenon is known as the non-Hermitian skin effect (NHSE). In early works, when the NHSE was discussed from the point of view of non-trivial topology, it was considered to be a failure of the conventional BEC [4]. More recently, it was shown that the 1D NHSE is indeed a topological phenomenon, and the location of the edge modes is predicted by the winding number of the bulk spectrum ~~[5]~~ [5–8]. In higher dimensions however, especially when eigenstate accumulation occurs at corners, multiple invariants have been proposed for different types of NHSE. A recent review has concluded that understanding the formation of corner skin modes is mostly done on a case-by-case basis, and that there is no current consensus on the general theoretical formalism behind it [9].

In the presence of impurities, the failure of the near-sightedness principle in non-Hermitian systems is further demonstrated. Non-Hermitian impurities are observed to attract the modes of the system with a localization length that is proportional to the

system size [10–13]. This phase is scale-invariant and is therefore considered distinct from the NHSE phase.

In this work, we show that an appropriately selected non-Hermitian impurity is capable of exponentially localizing all modes present in the system, thus challenging the association between the NHSE and ~~non-trivial topology~~BEC. We show that when translation symmetry is broken, the appearance of this effect as well as its position in real space becomes independent of any bulk topological index. This phenomenon occurs even when the bulk is fully Hermitian, further highlighting the breakdown of bulk-boundary correspondence and the near-sightedness principle. In the following, we explore these features using a simple one-dimensional (1D) model, highlighting first why this effect is expected to occur, followed by a concrete numerical demonstration. We then show this effect is also are present in a two-dimensional (2D) model.

The NHSE can be understood in terms of transfer matrices that relates the wave function at one boundary in a translationally invariant chain to the bulk wave function at a given energy E [14, 15]:

$$\begin{pmatrix}\psi(x_{N+1})\\ \psi(x_N)\end{pmatrix} = T_B^N(E)\begin{pmatrix}\psi(x_1)\\ \psi(x_0)\end{pmatrix}, \tag{1}$$

where $\psi(x_N)$ is the possibly multi-component wave function of the N-th unit cell, and $T_B(E)$ is the transfer matrix of one unit cell of the bulk of the chain. In non-Hermitian systems that host the NHSE, there is a preferred direction of transmission towards the boundary with the skin effect. The largest eigenvalue $\lambda_B(E)$ of the transfer matrix $T_B(E)$ representing transmission away from this boundary has a modulus smaller than 1, resulting in the largest eigenvalue of the transfer matrix $T_B^N(E)$ being $|\lambda_B^N(E)| \ll 1$. The magnitude of the eigenvalues of the transfer matrices are therefore directly linked to the accumulation of modes at a certain site: in non-Hermitian systems, they predict which boundary will host the NHSE.

Adding an impurity to the system modifies the transfer matrix. The transfer matrix relating the wave function components on the left side of the chain to those at an impurity on site $N+2$ is given by

$$T(N,E) = T_{\text{imp}}(E)T_B^N(E), \tag{2}$$

where $T_{\text{imp}}(E)$ is the transfer matrix between the wave function components $(\psi(x_N), \psi(x_{N-1}))^T$ and $(\psi(x_{N+1}), \psi(x_N))^T$. If $\lambda_{\text{imp}}(E)$, the smallest eigenvalue of the impurity transfer matrix $T_{\text{imp}}(E)$, is much larger than $\lambda_B^N(E)$, the largest eigenvalue of the bulk transfer matrix $T_B^N(E)$, then all of the modes of the system will accumulate at the impurity site instead of the boundary that hosts the NHSE. Therefore the condition for the NHSE to completely disappear from the system boundary is:

$$\min_E \ |\lambda_B^N(E)\lambda_{\text{imp}}(E)| \gg 1, \tag{3}$$

where E is any energy that lies within the boundary defined by the PBC eigenvalues of the ~~Hamiltonian~~Hamiltonian—or in other words within the point gap. Eq. (3) describes the case where all of the modes have shifted to the impurity, but the majority of the modes are likely displaced well below this condition. The lower bound on the impurity strength provided by Eq. (3) directly generalizes to the case when the bulk is disordered, in which case slowest decaying eigenvalue of the transfer matrix is replaced by the largest Lyapunov exponent of the system [16]. Alternatively, a weaker but more straightforwardly valid lower bound follows by minimizing $\lambda_B(E)$ over disorder realizations in addition to energy.

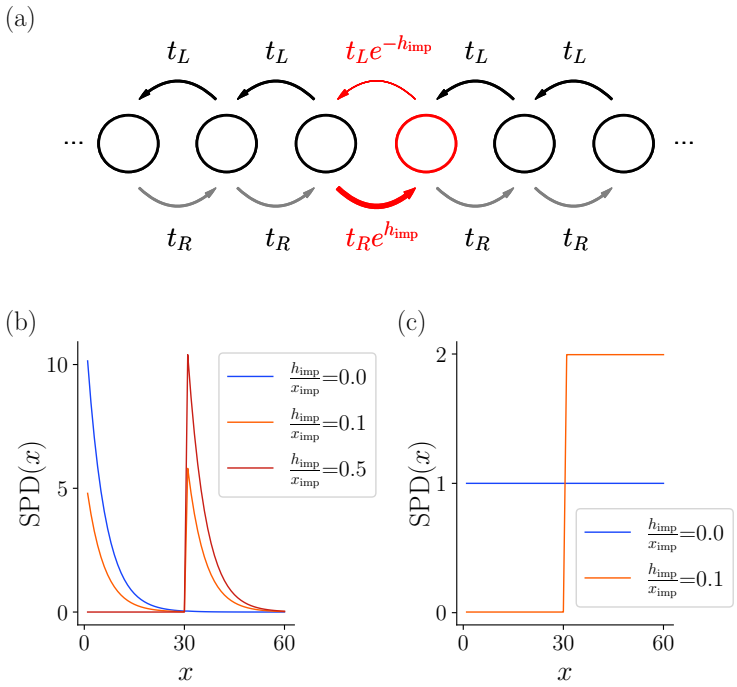

Figure 1: Breakdown of the correspondence of the skin effect and bulk topology via a non-Hermitian hopping impurity in the bulk, model Eq. (4). (a) Schematic of the tight-binding system Eq. (4) around the impurity site (in red). (b) The SPD [Eq. (5)] of a 1D chain of 60 sites in a non-Hermitian system ($t_R = 0.9$ and $t_L = 1.1$) with a non-Hermitian impurity located at $x_{\text{imp}} = 30$, as a function of increasing impurity strength h_{imp}. (c) Same as (b) for a Hermitian system ($t_R = 1$ and $t_L = 1$). Plot details in App. A.

As a concrete example, we now apply our reasoning to the Hatano-Nelson Hamiltonian [17,18], a 1D single-orbital non-Hermitian Hamiltonian:

$$\begin{aligned} H(m,N) = &\sum_{j\neq m}^{N} t_R|j\rangle\langle j-1| + t_L|j-1\rangle\langle j| \\ &+ e^{h_{\text{imp}}} t_R|m\rangle\langle m-1| + e^{-h_{\text{imp}}} t_L|m-1\rangle\langle m|, \end{aligned} \tag{4}$$

where the sum runs over the lattice sites j of the system, N is the total number of sites of the chain, m corresponds to the impurity site, and h_{imp} models the magnitude of the hopping asymmetry that defines the impurity [Fig. 1 (a)]. $h_{\text{imp}} = 0$ results in a uniform system with no impurity. For simplicity we do not consider onsite terms, and the non-Hermiticity of the bulk arises from the hopping asymmetry in the bulk, $t_R \neq t_L$.

We observe the effect of a non-Hermitian impurity in this model by tracking the spatial distribution of modes in the system, in order to determine its effect on the NHSE. An extensively used method of characterizing the NHSE is the calculation of the real-space sum of probability densities (SPD) of all eigenstates of a system:

$$\text{SPD}(x_j) = \sum_n |\Psi_n(x_j)|^2, \tag{5}$$

where $\Psi_n(x_j)$ is amplitude of the n-th eigenvector on site x_j. While the local density of states is defined for individual energies, the SPD is akin to a local density of states evaluated at all energies of the system. We set $t_L > t_R$. In doing so, we realize a

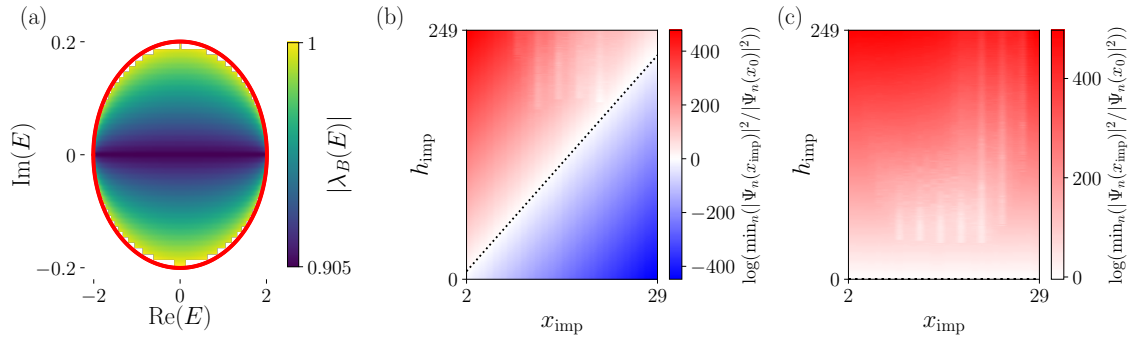

Figure 2: Breakdown of bulk-edge correspondence in a system with an amplifying non-Hermitian impurity, model Eq. (4). (a) The modulus of the largest eigenvalue of T_B [Eq. (6)] for all energies within the boundary defined by the PBC eigenvalues (in red), for $t_R = 0.9$ and $t_L = 1.1$. (b)-(c) the smallest ratio of eigenvector components at the impurity $|\Psi(x_{\text{imp}})|^2$ and the eigenvector components at the left boundary $|\Psi(x_0)|^2$ as a function of the impurity strength h_{imp} and impurity position x_{imp} for (b) non-Hermitian ($t_R = 0.0003$ and $t_L = 2980$) and (c) Hermitian systems ($t_R = 1$ and $t_L = 1$). The bound $|\lambda_B^{x_{\text{imp}}-2}(E)\lambda_{\text{imp}}(E)| = 1$ [Eq. (3)] is shown as a dotted line in (b) and (c), where E is the energy for which the modulus of the wave component at the impurity is the smallest. Plot details in App. A.

non-Hermitian system where the NHSE appears on the left of the chain, with modes exponentially localized around site $j = 0$. In non-Hermitian systems, as h_{imp} increases, the skin effect shifts away from the system boundaries to the impurity site in the bulk, as evidenced by the change in SPD [Fig. 1 (b)]. In Hermitian systems ($t_R = t_L = 1$), the non-Hermitian impurity depletes the modes to its left and accumulates them to its right [Fig. 1 (c)].

We now analyze the model Eq. (4) in terms of transfer matrices and the condition Eq. (3). We first examine the transfer matrix of the system without impurities. The transfer matrix relating wave functions of different unit cells in the bulk of the chain is given by:

$$T_B(E) = \begin{pmatrix} E/t_L & -t_R/t_L \\ 1 & 0 \end{pmatrix} \tag{6}$$

As shown in Fig. 2 (a), the modulus of the largest eigenvalue of $T_B(E)$ [Eq. (6)] is smaller than 1 for any energy that lies within the limits of the PBC spectrum. This means that the largest eigenvalue of the transfer matrix connecting increasingly distant points of the chain will be much smaller than 1.

We now consider the system with an impurity ($h_{\text{imp}} \neq 0$). The transfer matrix relating $(\psi(x_{\text{imp}}), \psi(x_{\text{imp}-1}))^T$ to $(\psi(x_{\text{imp}-1}), \psi(x_{\text{imp}-2}))^T$ is:

$$T_{\text{imp}}(E) = \begin{pmatrix} e^{h_{\text{imp}}} E/t_L & -e^{2h_{\text{imp}}} t_R/t_L \\ 1 & 0 \end{pmatrix}. \tag{7}$$

We diagonalize Eq. (4) for various hopping asymmetry strengths at the impurity located at x_{imp}, and extract the components of all the eigenvectors at the boundary $\Psi_n(x_0)$ and the components at the impurity site $\Psi_n(x_{\text{imp}})$. The smallest ratio of these components,

$$\min_n |\Psi_n(x_{\text{imp}})|^2 / |\Psi_n(x_0)|^2 \tag{8}$$

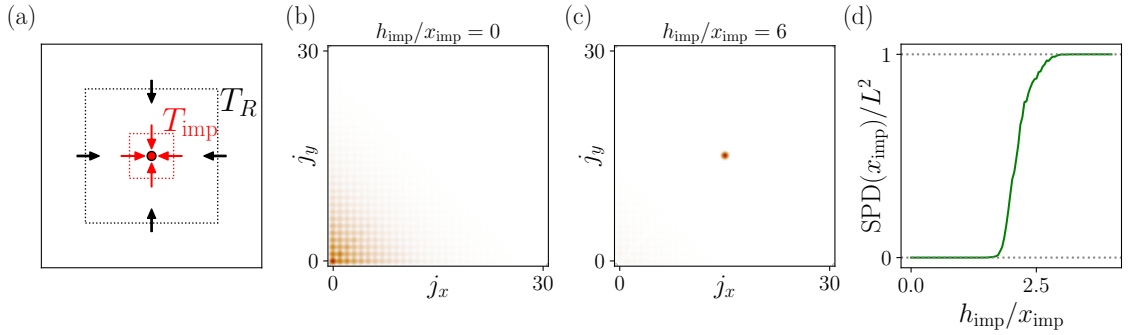

Figure 3: Shifting modes via a non-Hermitian impurity in a 2D non-Hermitian system hosting the NHSE. (a) Schematic of the 2D system with an impurity at the center. Black arrows indicate the direction of transfer operated by the rectangular transfer matrix T_R across the boundary marked by a black dashed line. Red arrows indicate the direction of transfer of the impurity transfer matrix T_{imp} across the boundary marked by the red dashed line. (b) SPD [Eq. (5)] of a 2D non-Hermitian system Eq. (9) with no impurities. Darker color indicates a larger SPD. (c) SPD of the same bulk non-Hermitian Hamiltonian with an impurity $h_{\text{imp}}/x\text{imp} = 6$. Darker color indicates a larger SPD. (d) SPD at the impurity site as a function of increasing impurity hopping asymmetry $h_{\text{imp}}/x_{\text{imp}}$, in a system with $t_L = t_U = e^1$ and $t_R = t_D = e^{-1}$. Plot details in App. A.

belongs to the eigenstate of the system that is the most localized at the boundary. With decreasing impurity distance from the boundary and/or increasing impurity strength, this ratio can be made arbitrarily large [Fig. 2 (b)], indicating that all of the modes of the system accumulate at the impurity for a large enough hopping asymmetry at the impurity. We also calculate $\lambda_B^{x_{\text{imp}}-2}(E)\lambda_{\text{imp}}(E)$, where E is the energy for which the modulus of the wave function at the impurity is the smallest. We use this expression to determine the threshold where the eigenvector most localized at the edge starts to shift towards the impurity, by plotting $\lambda_B^{x_{\text{imp}}-2}(E)\lambda_{\text{imp}}(E) = 1$. As shown in Fig. 2 (b), this threshold aligns with $\min_n |\Psi_n(x_{\text{imp}})|^2/|\Psi_n(x_0)|^2 = 1$, where the most localized eigenstate is equally present at the system boundary and at the impurity. For a fully Hermitian bulk ($t_R = t_L = 1$), the crossover threshold is located at $h_{\text{imp}} = 0$ [Fig. 2 (c)]. Fluctuations in $\min_n |\Psi_n(x_{\text{imp}})|^2/|\Psi_n(x_0)|^2$ present in Fig. 2 (b)-(c) are due to finite-size effects, see App. A.

We now extend our analysis to higher-dimensional systems. In a general d-dimensional system, we conjecture that a similar analysis can be performed by examining transfer matrices in the radial direction. We take 2D systems as an example [Fig. 3 (a)]. We consider the following 2D Hamiltonian:

$$\begin{aligned} H(m_x, m_y, N_x, N_y) = &\sum_{j_x \neq m_x}^{N_x} \sum_{j_y \neq m_y}^{N_y} t_R |j_x+1, j_y\rangle\langle j_x, j_y| + t_L |j_x, j_y\rangle\langle j_x+1, j_y| \\ &+ t_U |j_x, j_y+1\rangle\langle j_x, j_y| + t_D |j_x, j_y\rangle\langle j_x, j_y+1| \\ &+ e^{h_{\text{imp}}}(t_L |m_x, m_y\rangle\langle m_x+1, m_y| + t_R |m_x, m_y\rangle\langle m_x-1, m_y| \\ &\quad + t_D |m_x, m_y\rangle\langle m_x, m_y+1| + t_U |m_x, m_y\rangle\langle m_x, m_y-1|) \\ &+ e^{-h_{\text{imp}}}(t_L |m_x+1, m_y\rangle\langle m_x, m_y| + t_R |m_x-1, m_y\rangle\langle m_x, m_y| \\ &\quad + t_D |m_x, m_y+1\rangle\langle m_x, m_y| + t_U |m_x, m_y-1\rangle\langle m_x, m_y|) \end{aligned} \tag{9}$$

where the sums run over the coordinate indices of the lattice sites j_x, j_y of the system,

the impurity is located at $(j_x, j_y) = (m_x, m_y)$, and for simplicity we consider the hopping asymmetry at the impurity h_{imp} to be the same in both the x and y directions. There are four hopping asymmetry impurities, two to the immediate left and right of the impurity site, and two immediately above and below the impurity site.

In a one-dimensional chain, a transfer matrix argument connecting neighboring sites is sufficient to track the shifting of the modes towards an impurity [Fig. 2 (b)]. In two dimensions, we extend this argument to transfer matrices $T_R(E)$ that connect outer regions of a sample to its inner regions, following the example shown in Fig. 3 (a):

$$\boldsymbol{\psi}_{\text{in}} = T_R(E)\boldsymbol{\psi}_{\text{out}}, \tag{10}$$

where $\boldsymbol{\psi}_{\text{in}}$ are the wave components on the sites that lie immediately within the boundary denoted by the black dashed line, and $\boldsymbol{\psi}_{\text{out}}$ are the wave components on sites lying immediately outside the same boundary. Since the size of $\boldsymbol{\psi}_{\text{in}}$ is smaller than the size of $\boldsymbol{\psi}_{\text{out}}$, $T_R(E)$ is a rectangular matrix.

In the presence of an impurity at the center of a $N \times N$ lattice, the transfer matrix from the outer boundaries to the impurity is given by:

$$T(E) = T_1(E)T_2(E)\cdots T_{N/2-1}(E)T_{\text{imp}}(E), \tag{11}$$

where $T_i(E)$ are rectangular transfer matrices, and $T_{\text{imp}}(E)$ is the impurity transfer matrix as shown schematically in Fig. 3 (a). Since the radial transfer matrices are rectangular, there are wave functions at the edge of the system that inevitably have an exactly zero weight at the impurity. However, wave functions satisfying generic and not fine-tuned boundary conditions have weight in all the components, and therefore have a finite coupling to the impurity. Therefore we expect that in the general case, a non-Hermitian impurity that amplifies wave functions incoming from all directions should suppress all NHSE in a finite sample.

We now verify numerically that a non-Hermitian impurity in 2D is capable of attracting all of the modes in the system. We first consider the system with no impurity ($h_{\text{imp}} = 0$). We set $t_L = t_D = 1.1$ and $t_R = t_U = 0.9$, which results in a NHSE manifesting at the lower-left region of the 2D system [Fig. 3 (b)]. By then increasing h_{imp}, all of the modes of the system are attracted to the impurity [Fig. 3 (c)-(d)]. For Hermitian systems, a similar accumulation of system modes at the impurity site is observed to occur.

We have shown that local non-Hermitian perturbations draw the NHSE into the bulk of a system, which demonstrates the breakdown of BEC of the NHSE in 1D and 2D in the absence of translation symmetry. Predicting the position of the skin effect using topological invariants thus becomes unreliable once translation symmetry is broken. In real/non-ideal systems, translation symmetry is not guaranteed to be preserved, highlighting the importance of studying non-Hermitian systems in a manner that is sensitive to local details, such as wave packet dynamics [19], rather than bulk invariants.

The non-Hermitian impurities that we have considered here affect only a few hoppings, but they not purely local perturbations, in the sense that global information (the system size) is required in order to know how strong the hopping asymmetry at the impurity has to be before attracting all of the modes of the system.

Our work indicates that, owing to lack of a near-sightedness principle, impurities play a much larger role in non-Hermitian systems than they do in Hermitian ones. This may prove useful for experiments seeking to produce a non-Hermitian skin effect in a variety of material and meta-material systems [20–24]. Rather than tailor gain and loss or nonreciprocity throughout the entire bulk of the experimental system, a single, non-Hermitian local perturbation would be sufficient to generate the NHSE.

Data availability

The data shown in the figures, as well as the code generating all of the data is available at [25].

Author contributions

H. S. made the initial observation of non-Hermitian impurities attracting skin effect modes. H. S. performed the numerical simulations and wrote the manuscript with input from other authors. All authors contributed to the theoretical explanation behind this observation and defined the research plan.

Acknowledgments

A. A. and H. S. were supported by NWO VIDI grant 016.Vidi.189.180 and by the Netherlands Organization for Scientific Research (NWO/OCW) as part of the Frontiers of Nanoscience program. I. C. F. and V. K. acknowledge financial support from the DFG through the W urzburg-Dresden Cluster of Excellence on Complexity and Topology in Quantum Matter - ct.qmat (EXC 2147, project-id 390858490).

References

[1] W. Kohn, *Density functional and density matrix method scaling linearly with the number of atoms*, Phys. Rev. Lett. **76**, 3168 (1996), doi:10.1103/PhysRevLett.76.3168.

[2] E. Prodan and W. Kohn, *Nearsightedness of electronic matter*, Proceedings of the National Academy of Sciences **102**(33), 11635 (2005), doi:10.1073/pnas.0505436102.

[3] N. Okuma and M. Sato, *Non-hermitian topological phenomena: A review*, Annual Review of Condensed Matter Physics **14**(1), 83 (2023), doi:10.1146/annurev-conmatphys-040521-033133.

[4] Y. Xiong, *Why does bulk boundary correspondence fail in some non-hermitian topological models*, J. Phys. Commun. **2** (2018), doi:10.1088/2399-6528/aab64a.

[5] N. Okuma, K. Kawabata, K. Shiozaki and M. Sato, *Topological origin of non-hermitian skin effects*, Physical Review Letters **124**(8) (2020), doi:10.1103/physrevlett.124.086801.

[6] K. Kawabata, K. Shiozaki, M. Ueda and M. Sato, *Symmetry and topology in non-hermitian physics*, Phys. Rev. X **9**, 041015 (2019), doi:10.1103/PhysRevX.9.041015.

[7] Z. Gong, Y. Ashida, K. Kawabata, K. Takasan, S. Higashikawa and M. Ueda, *Topological phases of non-hermitian systems*, Phys. Rev. X **8**, 031079 (2018), doi:10.1103/PhysRevX.8.031079.

[8] S. Yao and Z. Wang, *Edge states and topological invariants of non-hermitian systems*, Phys. Rev. Lett. **121**, 086803 (2018), doi:10.1103/PhysRevLett.121.086803.

[9] X. Zhang, T. Zhang, M.-H. Lu and Y.-F. Chen, *A review on non-hermitian skin effect*, Advances in Physics: X **7**(1), 2109431 (2022), doi:10.1080/23746149.2022.2109431.

[10] L. Li, C. H. Lee and J. Gong, *Impurity induced scale-free localization*, Communications Physics **4**(1) (2021), doi:10.1038/s42005-021-00547-x.

[11] C.-X. Guo, X. Wang, H. Hu and S. Chen, *Accumulation of scale-free localized states induced by local non-hermiticity*, arXiv preprint (2023), doi:10.48550/ARXIV.2302.02798.

[12] B. Li, H.-R. Wang, F. Song and Z. Wang, *Scale-free localization and pt symmetry breaking from local non-hermiticity*, arXiv preprint (2023), doi:10.48550/ARXIV.2302.04256.

[13] P. Molignini, O. Arandes and E. J. Bergholtz, *Anomalous skin effects in disordered systems with a single non-hermitian impurity*, arXiv preprint (2023), doi:10.48550/arXiv.2302.09081.

[14] F. K. Kunst and V. Dwivedi, *Non-hermitian systems and topology: A transfer-matrix perspective*, Phys. Rev. B **99**, 245116 (2019), doi:10.1103/PhysRevB.99.245116.

[15] L. Molinari, *Transfer matrices, non-hermitian hamiltonians and resolvents: some spectral identities*, Journal of Physics A: Mathematical and General **31**(42), 8553 (1998), doi:10.1088/0305-4470/31/42/014.

[16] K. Kawabata and S. Ryu, *Nonunitary scaling theory of non-hermitian localization*, Phys. Rev. Lett. **126**, 166801 (2021), doi:10.1103/PhysRevLett.126.166801.

[17] N. Hatano and D. R. Nelson, *Localization transitions in non-hermitian quantum mechanics*, Phys. Rev. Lett. **77**, 570 (1996), doi:10.1103/PhysRevLett.77.570.

[18] N. Hatano and D. R. Nelson, *Vortex pinning and non-hermitian quantum mechanics*, Phys. Rev. B **56**, 8651 (1997), doi:10.1103/PhysRevB.56.8651.

[19] H. Spring, V. Könye, F. A. Gerritsma, I. C. Fulga and A. R. Akhmerov, *Phase transitions of wave packet dynamics in disordered non-hermitian systems*, arXiv preprint (2023), doi:10.48550/ARXIV.2301.07370.

[20] A. Wang, Z. Meng and C. Q. Chen, *Non-hermitian topology in static mechanical metamaterials*, Science Advances **9**(27), eadf7299 (2023), doi:10.1126/sciadv.adf7299, https://www.science.org/doi/pdf/10.1126/sciadv.adf7299.

[21] C. Scheibner, W. T. M. Irvine and V. Vitelli, *Non-hermitian band topology and skin modes in active elastic media*, Phys. Rev. Lett. **125**, 118001 (2020), doi:10.1103/PhysRevLett.125.118001.

[22] R. Cai, Y. Jin, Y. Li, T. Rabczuk, Y. Pennec, B. Djafari-Rouhani and X. Zhuang, *Exceptional points and skin modes in non-hermitian metabeams*, Phys. Rev. Appl. **18**, 014067 (2022), doi:10.1103/PhysRevApplied.18.014067.

[23] A. Ghatak, M. Brandenbourger, J. van Wezel and C. Coulais, *Observation of non-hermitian topology and its bulk–edge correspondence in an active mechanical metamaterial*, Proceedings of the National Academy of Sciences of the United States of America **117**(47), pp. 29561 (2020).

[24] L. Cao, Y. Zhu, S. Wan, Y. Zeng and B. Assouar, *On the design of non-hermitian elastic metamaterial for broadband perfect absorbers*, International Journal of Engineering Science **181**, 103768 (2022), doi:https://doi.org/10.1016/j.ijengsci.2022.103768.

[25] H. Spring, V. Konye, A. R. Akhmerov and I. C. Fulga, *Lack of near-sightedness principle in non-hermitian systems*, doi:10.5281/zenodo.8204845 (2023).

A Model and plotting parameters

In this section additional details of the plots are listed in order of appearance.

For Fig. 1, simulations were done for 1D systems composed of 60 sites. The values of h_{imp} used are 0, $0.05L$, and $0.25L$, for both the non-Hermitian and the Hermitian systems. For panel (b), the bulk Hamiltonian parameters are $t_L = e^{0.1} = 1.1$ and $t_R = e^{-0.1} = 0.9$. For panel (c), the bulk Hamiltonian parameters are $t_L = 1$ and $t_R = 1$.

For Fig. 2 (a), simulations were done for 1D systems composed of 10 sites. For the non-Hermitian system shown in panel (b), bulk parameters $t_L = e^8$ and $t_R = e^{-8}$ were used. The high hopping asymmetry in the bulk is used to reduce the oscillations of $\min_n |\Psi_n(x_{\text{imp}})|^2/|\Psi_n(x_0)|^2$ that arise due to the penetration of the skin effect into the bulk (as shown for example in Fig. 1 (b)). Parameters $t_L = 1$ and $t_R = 1$ were used for the Hermitian system shown in panel (c).

For Fig. 3, simulations shown in panels (b)-(d) were performed using 2D systems composed of 31×31 sites with bulk hopping parameters $t_L = t_U = e^1$ and $t_R = t_D = e^{-1}$ (see (9)). In panels (b) and (c), the impurity hopping asymmetry is $h_{\text{imp}}/x_{\text{imp}} = 0$ in (b) and $h_{\text{imp}}/x_{\text{imp}} = 6$ in (c).